Climate
of the Past
Discussions
Open Access
EGU

Climate change drove Late Miocene to Pliocene rise and fall of C4 vegetation at the crossroads of Africa and Eurasia (Anatolia, Türkiye)

Maud J.M. Meijers[1,2*], Tamás Mikes[2,3], Bora Rojay[4], H. Evren Çubukçu[5], Erkan Aydar[5], Tina Lüdecke[2,6], Andreas Mulch[2,7]

[1]Department of Earth Sciences, NAWI Graz Geocenter, University of Graz, Heinrichstraße 26, 8010 Graz, Austria

[2]Senckenberg Biodiversity and Climate Research Centre, Senckenberganlage 25, 60325 Frankfurt am Main, Germany

[3]Independent geological consultant, Arnljot Gellines vei 35, 0657 Oslo, Norway

[4]Department of Geological Engineering, Middle East Technical University, 06800 Çankaya, Ankara, Türkiye

[5]Department of Geological Engineering, Hacettepe University, Beytepe Campus, 06800 Ankara, Türkiye

[6]Emmy Noether Group for Hominin Meat Consumption, Max Planck Institute for Chemistry, Hahn-Meitner-Weg 1, 55128 Mainz, Germany

[7]Institute of Geosciences, Goethe University Frankfurt, Altenhöferallee 1, 60438 Frankfurt am Main, Germany

Correspondence to: Maud Meijers (maud.meijers@uni-graz.at)

Abstract. Life on Earth has been capitalizing on the C_3 photosynthetic pathway for 2.8 billion years. However, in the world's grasslands that emerged since the Paleogene, C_4 vegetation expanded dramatically between 8 and 3 Ma in response to climatic changes. Here we present the first comprehensive Late Miocene to Holocene $\delta^{13}C$ soil carbonate record from the Eastern Mediterranean region (Anatolia) to reconstruct long-term geographic distributions of C_3 and C_4 plants, a region with patchy records compared to parts of Africa and Asia. Our results show a colonization of Anatolian floodplains by C_4 biomass by 9.9 Ma, similar to regions in NW and E Africa, followed by a transition from this mixed C_3-C_4 vegetation to C_4 dominance between ca. 7.1 Ma and 4.9 Ma. The transition coincides with a similar shift from C_3 to C_4 vegetation in southern Asia and is generally attributed to the Late Miocene Cooling in response to decreasing atmospheric pCO_2. However, the Anatolian paleoecosystem patterns are unique due to a rapid and permanent return to C_3 dominance in the Early Pliocene, which is not observed elsewhere and occurs simultaneously with the disappearance of the open environment-adapted large mammal Pikermian chronofauna. We propose that this return to C_3 vegetation was caused by paleoclimatic processes that regionally shifted precipitation from the warm to the cool season, resembling the modern Mediterranean climate. In conclusion, changes in rainfall seasonality under subhumid climate, rather than increased aridity, drove the demise of C_4-dominated floodplains and the open-environment adapted Pikermian chronofauna at the Eurasian-African crossroads.

Climate
of the Past
Discussions

1. Introduction

The earliest grassland ecosystems that emerged in the Paleogene were occupied by vegetation using the C_3 oxygenic photosynthetic pathway (Strömberg, 2011). However, many of the grassland environments that occupy ca. 40 % of Earth's

35 landmass today are dominated by C_4 vegetation, including the Great Plains of North America, eastern South America, sub-Saharan Africa, southeast Asia, and northern Australia (Still et al., 2003). C_4 biomass consists of grasses (ca. 60 %), sedges, and dicots, and is adapted to conditions of drought, low atmospheric pCO_2, and high temperatures (Sage, 2004). Although C_4 vegetation has been present since the Oligocene (Peppe et al., 2023; Urban et al., 2010), the rise to dominance of C_4 at the expense of C_3 vegetation in much of the world's grassland environments was delayed until the Late Miocene or even the

40 Pliocene (Edwards et al., 2010; Strömberg, 2011).

Figure 1: Topographic map of the Anatolian-Aegean region including sampling sites from this study and published studies in the Aegean (Greece) and Anatolia (Türkiye). Circles: this study; hexagon Meijers et al. (2018); star: Lepetit (2010); diamonds: Böhme et al. (2017); triangles: Quade et al. 1994). Geographic sampling areas correspond to those in Supplementary Table S1 and S3. CAVP= Central Anatolian

45 Volcanic Province. Inset: Map of the Old World; red box refers to Anatolian-Aegean region.

Grassland expansion led to the evolution of open environment-adapted and hypsodont large herbivorous mammal communities of the Old World savannah paleobiome (OWSP) in Asia, East Africa, and southern Europe during the Late Miocene (Kaya et al., 2018) until its Early Pliocene fragmentation (Böhme et al., 2021). The western Eurasian branch of the

50 OSWP, the Pikermian chronofauna, reached its greatest geographic extent around ca. 8.0−6.6 Ma-ago and occupied large parts of Europe and Central Asia, including Anatolia (Eronen et al., 2009) when C_4 vegetation became dominant in certain grasslands of the Old World. Reconstructing the spread of C_4 vegetation through geologic time is crucial for identifying the global and

regional climatic drivers behind faunal turnover, including the spread and decline of the Pikermian chronofauna. Direct evidence for the presence of C_4 vegetation in southern Europe and the Turkish-Iranian plateau region, however, is spatially

55   and temporally patchy and incomplete (Böhme et al., 2017; Butiseacă et al., 2022; Urban et al., 2010).

Here, we reconstruct proportions of C_4 biomass in south-central Anatolia (Türkiye; Fig. 1), which is crucially located at the crossroads of well-studied regions in terms of vegetation dynamics in Africa and Asia (Behrensmeyer et al., 2007; Uno et al., 2011). We analyze carbon isotopic compositions ($\delta^{13}C$) of ca. 10 Ma to Holocene pedogenic carbonates from Anatolia. Based on the fundamentally different fractionation of carbon isotopes during photosynthesis of C_3 ($\delta^{13}C= -26.7 \pm 12.3$ ‰)

60   and C_4 vegetation ($\delta^{13}C= -12.5 \pm 1.1$ ‰, Cerling et al., 1997) the transfer of this signal into materials such as pedogenic carbonates, mammalian tooth enamel, or leaf waxes can be used to reconstruct contributions of C_4 vegetation in deep time (Tipple and Pagani, 2007).

Our results of 447 pedogenic carbonate samples from sixteen sites show that C_4 plants spread within Anatolia by 9.9 Ma and rose to ecological dominance before 7.3 Ma (Fig. 2), a timing similar to that of southern Asian locations (Quade and

65   Cerling, 1995) and consistent with the few (64 samples from twelve sites) available Aegean (Greece) soil carbonate $\delta^{13}C$ records (Böhme et al., 2017; Quade et al., 1994). The rise of C_4 vegetation in Anatolia occurred simultaneously with the spread of the Pikermian chronofauna. The uniqueness of our dataset when compared to Asian and African records lies in the rapid and persistent decline of C_4 biomass between 4.9 and 3.9 Ma, after which Anatolia was again dominated by C_3 plants. This Anatolian demise of C_4 vegetation coincides within uncertainty with the disappearance of the hypsodont Pikermian

70   chronofauna, suggesting a common driver. In contrast to the continuing dominance of C_4 grasslands in other parts of the world, we propose that regional climatic changes led to the fall of C_4 vegetation in Anatolia and perhaps the Aegean. Given that most regions worldwide presently dominated by C_4 vegetation display not only pronounced wet and dry seasons but also warm season precipitation, we suggest that a change from warm to cold season precipitation led to the establishment of the present-day Mediterranean-style climate, fostered the demise of C_4 vegetation, and the extinction of the Pikermian chronofauna in the

75   region.

2.   Material and methods

2.1 Pedogenic carbonates sampling

In Anatolia, eight pedogenic carbonate sites were sampled within the Central Anatolian Volcanic Province (CAVP) and two

80   sites each adjacent to the Tuz Gölü and Ecemiş fault zones, as well as the Ermenek basin. Two additional sites were sampled within the Adana basin near the Mediterranean Sea (Fig. 1b; see Supplementary Table S1 for detailed site information). Site elevations range between ca. 110 m and 1650 m a.s.l. and the sampled soil carbonates range in age from ca. 10 Ma to modern (Fig. 1b; Supplementary Table S1). Holocene pedogenic carbonate samples consist of friable to weakly consolidated calcareous nodules typically 1 to 3 cm in diameter, from the B horizon of well-drained soils with a pink to red hackly

85   appearance. Miocene to Pleistocene carbonate subsoil horizons developed within floodplain deposits. They comprise moderately consolidated to hard calcareous nodules ranging from 3 to 8 cm in diameter, or representative domains of dm-scale

nodular carbonate layers. Whenever possible, pedogenic carbonate nodules and in some cases casts of taproots and fibrous roots, were collected from Bk horizons of cream to red-colored subsurface soils. Where identifiable, pedogenic carbonate was sampled at a minimum soil depth of 30 cm to reduce the influence of atmospheric CO_2 (Cerling and Quade, 1993).

90

2.2 δ¹³C of pedogenic carbonates

Powdered sample material from pedogenic carbonate nodules was extracted with a diamond-tip dental drill. A total of 447 $\delta^{13}C$ values were obtained for pedogenic carbonate samples from sixteen sites at the joint Goethe University-Senckenberg Biodiversity and Climate Research Centre Stable Isotope Facility in Frankfurt (Germany). Multiple measurements were

95 performed on single pedogenic carbonate nodules which were cross-sectioned from three sites: 10TG55 (n= 16, five nodules, three to four analyses per nodule), 10FD (n= 48, 25 nodules, of which three nodules with six to 13 analyses per nodule), and 12C047−052 (n= 24, 16 nodules, of which two nodules with five measurements each; Supplementary Table S1). Powdered carbonate samples were digested in 98 % H_3PO_4 and analyzed as CO_2 in continuous flow mode using a Thermo MAT 253 mass spectrometer interfaced with a Thermo GasBench II. Analytical procedures followed those of Spötl and Vennemann

100 (Spötl and Vennemann, 2003). Raw isotopic ratios were calibrated against an in-house standard (Carrara marble) and international carbonate reference materials (NBS18 and NBS19). Final isotopic ratios are reported against Vienna Pee Dee Belemnite (V-PDB), with analytical uncertainties that are typically better than 0.07 ‰. Standard deviations for all average $\delta^{13}C$ values refer to 1σ uncertainties. Pedogenic carbonate that formed in equilibrium with soil-respired CO_2 is enriched by ca. 14-17 ‰ in $\delta^{13}C$ compared to CO_2 derived from root respiration and microbial decomposition of organic matter (e.g., Tipple

105 and Pagani, 2007).

2.3 Pedogenic carbonate chronology

Age constraints for the paleosols containing the analyzed pedogenic carbonates from the CAP and the Tuz Gölü area are based on the radiometrically dated ignimbrite intercalations of the CAVP (Aydar et al., 2012; Özsayin et al., 2013). The stratigraphic

110 framework for the sampled horizons is based on the ignimbrite stratigraphy and the published geochronological data (see Supplementary Table S1). The Quaternary age for site 11AD is based on the 1:500,000 geological map of Adana (Ulu, 2002). Modern soil carbonate horizons were identified based on field relationships and assigned a Holocene age (5 ± 5 ka).

2.4 Reconstruction of climatic parameters

115 A reconstruction of paleobotany-derived climatic parameters of Anatolia (Fig. 2b, c) is based on the coexistence approach (Mosbrugger and Utescher, 1997). All data are listed in Supplementary Table S2.

2.5 Compilation of δ¹³C values from Old World soil carbonates

The compilation of 12 Ma to Holocene soil carbonate $\delta^{13}C$ values from Türkiye and Greece (Fig. 2a; Supplementary Table

120 S3) includes data from Böhme et al. (2017), Lepetit (2010), and Quade et al. (1994).The compilation of 12 Ma to Holocene

soil carbonate δ^{13}C values from Asia and Africa (Fig. 3d, e) was retrieved from Fox et al. (2018). Datasets lacking age constraints were excluded, along with data from a publication on the Qaidam basin that report elevated δ^{13}C values atttributed to increased aridification (Zhuang et al., 2011). Studies included in the Africa compilation (Fig. 3e): Aronson et al., (2008), Bestland and Krull (1999), Cerling and Hay (1986), Cerling et al. (1988, 1991, 2003, 2011), Kingston (1992), Levin et al.

125 (2004, 2011), Plummer et al. (1999, 2009), Quade et al. (2004), Quinn et al. (2007), Sahnouni et al. (2011), Sikes (1994), Sikes et al. (1999), Sikes and Ashley (2007), WoldeGabriel et al. (2009), Wynn (2000, 2004), Wynn et al. (2006). Studies included in the Asia compilation (Fig. 3d): Behrensmeyer et al. (2007), Ding and Yang (2000), Ghosh et al. (2004), Kaakinen et al. (2006), Passey et al. (2009), Quade et al. (1994), Quade and Cerling (1995), Sanyal et al. (2004), Yao et al. (2010), An et al, (2005).

130

3. Results

δ^{13}C values from the sixteen 10 Ma to Holocene sampled soil carbonate locations range from −9.5 to 3.4 ‰, with an average of −5.4 ± 3.4 ‰ (Supplementary Table S1). Based on their δ^{13}C values, we categorize the pedogenic carbonate record into four time intervals:

135 **9.9 Ma:** δ^{13}C values of a single 9.9 Ma site (Mustafapaşa, n= 24, age: 9.88 ± 0.75 Ma) in the Central Anatolian Volcanic Province (CAVP) range from −8.0 to 2.5 ‰, with an average of −5.2 ± 2.6 ‰.

7.1 to 4.9 Ma: The average δ^{13}C value for the six sections (n= 154) from the CAVP is −1.2 ± 2.0 ‰, which is ca. 4 ‰ more positive than the 9.9 Ma Mustafapaşa dataset. At Orta Tepe South (n= 22, 7.05 ± 0.15 Ma) δ^{13}C values range from −4.8 to 1.5 ‰, with an average of −1.1 ± 2.1 ‰. At Taşkınpaşa South (n= 6, 6.21 ± 0.14 Ma) δ^{13}C values range from −5.7 to 0.7 ‰, with

140 an average of −1.6 ± 2.6 ‰. Orta Tepe West was sampled near Taşkınpaşa South between the same two ignimbrites and thus covers the same age interval (n= 22, 6.21 ± 0.14 Ma). δ^{13}C values range between −5.8 and 2.7 ‰, with an average of −2.5 ± 2.0 ‰. At Şahinefendi (n= 86, 5.68 ± 0.66 Ma) δ^{13}C values range from −5.6 to 2.7 ‰ with an average of −1.3 ± 1.6 ‰. At Taşkınpaşa Southwest (n=3, 5.68 ± 0.66 Ma) δ^{13}C values range from −0.8 to 1.4 ‰ with an average of 0.1 ± 1.1 ‰ whereas at Güzelöz (n= 15, 4.86 ± 0.16 Ma) δ^{13}C values range from −3.9 to 3.4 ‰, with an average of 1.0 ± 2.1 ‰.

145 **3.9 Ma to 1.4 Ma:** Three pedogenic carbonates sites were sampled in the southern part of the CAP (CAVP and Tuz Gölü fault (TGF)), the Tauride Mountains (Ecemiş fault zone (EFZ) and Ermenek basin), and the Adana basin. The average δ^{13}C value (n= 188) is −7.7 ± 0.8 ‰, which is nearly 7 ‰ more negative than the 7.1 to 4.9 Ma dataset. At Cerit near the TGF (n = 96, 3.86 ± 0.20 Ma) δ^{13}C values range from −8.3 to −4.7 ‰, with an average of −7.2 ± 0.5 ‰. Similarly, Taşhan (CAVP, n= 3, 3.81 ± 1.08 Ma) yields δ^{13}C values between −8.0 and −7.0 ‰ (average: −7.4 ± 0.5 ‰). Baklalı/Misis (Adana basin, n= 89,

150 1.35 ± 1.25 Ma) yields δ^{13}C values between −9.2 and −6.5 ‰ with an average of −8.2 ± 0.6 ‰.

Holocene (5 ± 5 ka) δ^{13}C values from the six sections containing Holocene soil carbonates (n= 87) average −8.1 ± 1.0 ‰, which is within uncertainty identical to the 3.9 to 1.4 Ma datasets. Individual sites yield the following δ^{13}C values: Gildirli (Adana basin, n= 6) −9.0 to −4.6 ‰ with an average of −7.4 ± 2.1 ‰; Fındıklı (EFZ, n= 48) −9.3 to −7.6 ‰ with an average of −8.4 ± 0.4 ‰; Bulanlık (EFZ, n= 12) −7.2 to −5.5 ‰ with an average of −6.3 ± 0.6 ‰; Altınkaya (TGF, n= 16) −8.6 to −8.3

155 ‰ with an average of −8.5 ± 0.1 ‰; Güneyyurt (Ermenek basin, n= 3) −9.5 to −8.1 ‰ with an average of −8.8 ± 0.7 ‰, and Yalındal (Ermenek basin, n= 2) with values of −9.3 ‰ and −8.7 ‰.

In summary, all soil carbonates younger than ca. 3.9 Ma yield nearly 7 ‰ lower $\delta^{13}C$ values than the 7.1 to 4.9 Ma soil carbonates, as well as ca. 2.5 ‰ lower $\delta^{13}C$ values than the ca. 9.9 Ma-old soil carbonate dataset (Fig. 2).

160 ## 4. Discussion

4.1 Soil carbonate $\delta^{13}C$ reveals variations of C₃ and C₄ vegetation in Anatolia and the Aegean

The 12 Ma to Holocene $\delta^{13}C$ record from Anatolia shows large changes between the four time intervals (see Sect. 3 Results) and covers a wide range from −9.5 ‰ to 3.4 ‰ (Fig. 2). This variation in $\delta^{13}C$ values (up to 12.9 ‰) may reflect temporal changes in soil respiration rates, plant water stress, and/or the dominating photosynthetic pathway (C₃ vs. C₄) of biomass in

165 Anatolia. $\delta^{13}C$ values within our Anatolian dataset display a large variation (up to 12.9 ‰) of soil carbonate. We interpret obtained $\delta^{13}C$ values as primary (i.e. reflecting the $\delta^{13}C$ values upon the formation of the carbonates), because the values are within a range typical of soil carbonates (e.g., Cerling and Quade, 1993) and because the soil carbonate samples and their fluvio-lacustrine host lithologies show no evidence of diagenetic alteration. Moreover, all sites except one (Mustafapaša, ca. 9.9 ± 0.8 Ma) within the Central Anatolian Plateau interior were buried only 170 m or less (Supplementary Table S1) due to

170 relatively low sedimentation rates (ca. 25−80 m/Myr; Supplementary Table S1) and rapid drainage integration and incision of the basins within maximal 2.5 Myrs after the latest deposition of the soil carbonate host lithologies (Brocard et al., 2021; Meijers et al., 2020).

Under conditions of low soil CO_2 production, soil carbonates tend to form at shallower depths and may incorporate varying proportions of atmospheric CO_2 (Cerling, 1984; Cerling and Quade, 1993), resulting in higher $\delta^{13}C$ values (Caves et al., 2016;

175 Licht et al., 2020). Particularly in dry ecosystems, C₃ plants may yield increased $\delta^{13}C$ values (Kohn, 2010). Although Anatolia is presently characterized by a climate with dry summers, all available paleobotanic datasets from the region suggest subhumid climatic conditions during the Late Miocene to Pliocene (Supplementary Table S2). We therefore interpret the variations in $\delta^{13}C$ values of our 10 Ma to recent soil carbonate record to reflect significant changes in the relative contribution of C₃ and C₄ components of vegetation.

180 The large range of soil carbonate $\delta^{13}C$ values of over 10 ‰ at ca. 9.9 Ma in Anatolia is consistent with a heterogeneous vegetation cover that includes both C₃ and C₄ plants, albeit with a dominance of C₃ vegetation given an average $\delta^{13}C$ of −5.2 ‰. Pedogenic carbonate $\delta^{13}C$ values between 7.1 and 4.9 Ma, which average 4.0 ‰ more positive compared to $\delta^{13}C$ values at 9.9 Ma indicate central Anatolian floodplain environments dominated by C₄ vegetation (Fig. 2a). The dominance of C₄ biomass between 7.1 and 4.9 Ma is consistent with published CAP $\delta^{13}C$ values of pedogenic carbonate from this time interval (6.7 to

185 4.8 Ma; Fig. 2a; (Lepetit, 2010)), some of which were obtained from the same stratigraphic intervals. For the time intervals from 3.9 to 1.4 Ma and the Holocene our $\delta^{13}C$ averages are significantly lower – by nearly 7 ‰ – than those from the 7.1 to 4.9 Ma interval, and by ca. 2.5 ‰ compared to the 9.9 Ma interval. This indicates the presence of floodplains dominated by C₃ vegetation after 3.9 Ma.

Climate
of the Past
Discussions
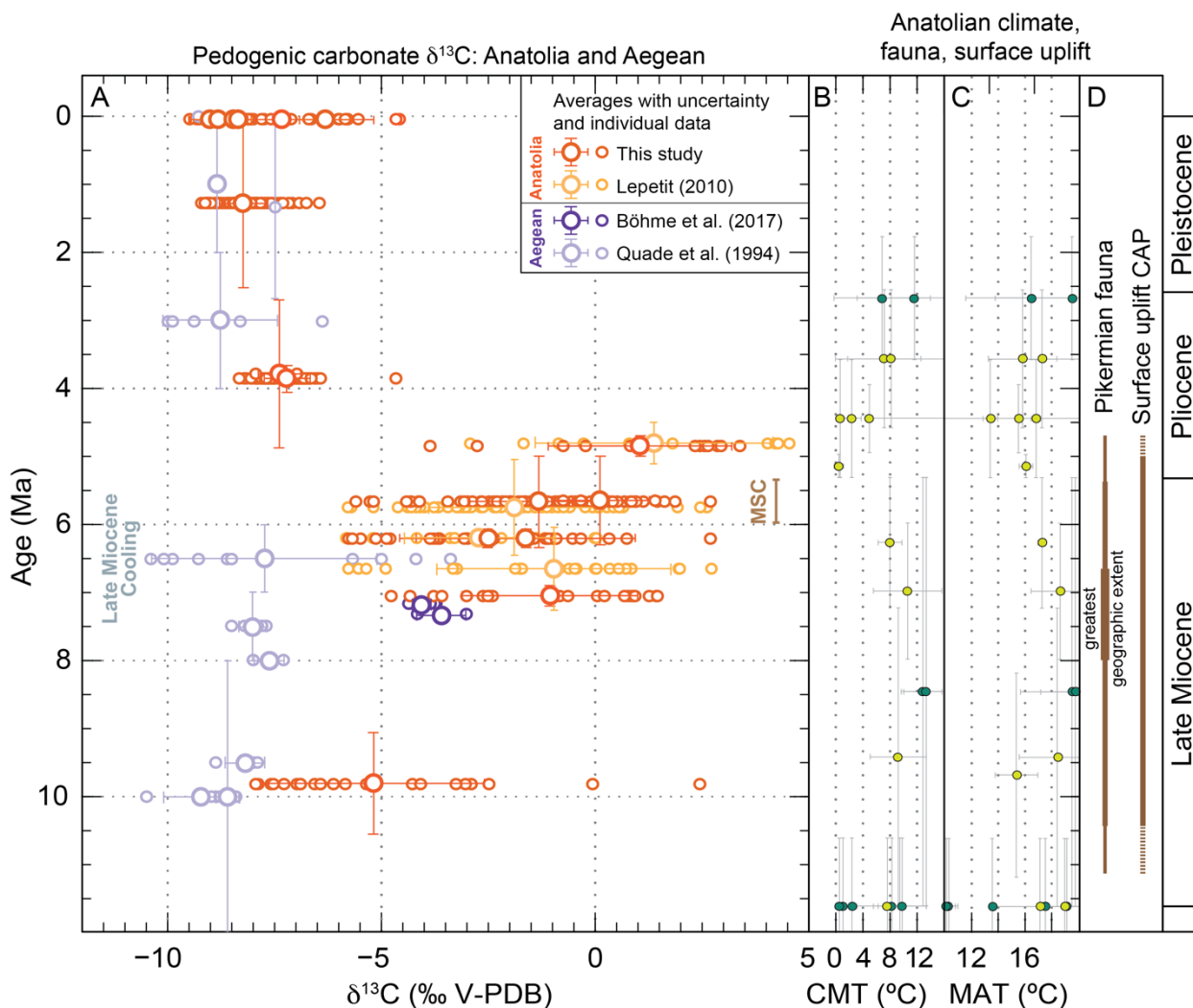
Figure 2: 12 to 0 Ma Anatolian and Aegean pedogenic carbonate δ^{13}C records and Anatolian climatic, faunal, and surface uplift records. (a) Pedogenic carbonate δ^{13}C values and their averages per site for this (orange) and published (purple, yellow) studies ((Böhme et al., 2017; Lepetit, 2010; Meijers et al., 2018; Quade et al., 1994) from the Anatolian-Aegean region. Global 'Late Miocene Cooling' (blue shading) according to Herbert et al. (2016). MSC: Messinian Salinity Crisis. (b) and (c): Published paleobotanical data-based (Supplementary Table S2) cold month mean temperature (CMT) and mean annual temperature (MAT) reconstructions for Anatolia. Light green circles indicate sites that are currently within in the CAP interior (ca. 1−1.5 km elevation), dark green circles indicate (near-)coastal sampling sites. (d) Periods during which the Pikermian chronofauna roamed Anatolia and surface uplift of the CAP occurred (onset: ca. 11 Ma; (Meijers et al., 2018)). The greatest geographic extent refers to the western Eurasian distribution of the Pikermian fauna (Eronen et al., 2009).

δ^{13}C values of ca. 9.3 to 5.3 Ma fossil equid tooth enamel (Rey et al., 2013), and ca. 10 to 6.5 Ma pedogenic carbonate δ^{13}C records (Böhme et al., 2017; Quade et al., 1994; Supplementary Table S3) from the Aegean region indicate C_3 vegetation.

However, phytoliths, as well as $\delta^{13}C$ values of published pedogenic carbonate and fossil herbivore tooth enamel, imply the presence of C_4 vegetation between ca. 9 Ma and 7 Ma in the CAVP (Kayseri-Özer et al., 2017; Lepetit, 2010), Pikermi and Samos (Aegean, Greece; Fig. 1b; Böhme et al., 2017; Quade et al., 1994), and Maragheh (Bernor et al., 2016; Biasatti et al., 2015; Strömberg et al., 2007). On Crete and Cyprus ca. 5 ‰ variations in $\delta^{13}C$ values of leaf waxes (long-chain n-alkanes

205 produced by terrestrial plants), superimposed on an overall 4 ‰ increase in $\delta^{13}C$ values between ca. 7 and 6 Ma, indicate the expansion of C_4 vegetation (Butiseacă et al., 2022; Mayser et al., 2017) in response to Messinian climate cycles. Collectively, our data in combination with published datasets indicate that the geographic extent of C_4 expansion in the Eastern Mediterranean region during the Late Miocene and earliest Pliocene may not have been restricted to Anatolia, but extended into the Aegean and the Iranian plateau. After 3.9 Ma (late Early Pliocene), $\delta^{13}C$ values from Anatolian soil carbonates are

210 similar to those derived from the Aegean (Quade et al., 1994) Fig. 1b) and indicate vegetation dominated by C_3 biomass, which is the observed dominant vegetation type in Anatolia and the Aegean region today (< 10 % C_4; Still et al., 2003).

4.2 Late Miocene to Pliocene circum-Anatolian ecosystem reconstructions

Pedogenic carbonates from ca. 10 Ma to Holocene floodplain deposits in Anatolia indicate that the region has been
215 characterized by rainfall seasonality since the Late Miocene, as their formation requires periodic soil drying (e.g., Zamanian et al., 2016). Furthermore, the dominance of C_4 vegetation between 7.1 and 4.9 Ma in Anatolia, as reconstructed from our pedogenic carbonate $\delta^{13}C$ values, suggests that open-habitat grasslands characterized major portions of the landscape. This is supported by a) paleobotanical (macrofossils, pollen, and spores) data that suggest the introduction of steppe elements in Anatolia between 9 and 6 Ma (Denk et al., 2018), b) the (Middle-)Late Miocene rise of open-habitat grasslands in Anatolia
220 and nearby Greece and Iran (Strömberg et al., 2007) reconstructed from phytoliths, and c) the presence of the open-environment adapted Pikermian chronofauna in those regions (Eronen et al., 2009). Simultaneously, however, macrofossil, pollen, and spore records from Anatolia, Greece, and Bulgaria (Denk et al., 2018) sketch Late Miocene landscapes dominated by evergreen needleleaf forests and mixed forests. We propose that the seemingly contradictory datasets reflect heterogeneous Late Miocene Anatolian landscapes with largely interconnected forested and savannah-like environments (Fortelius et al., 2019), which finds
225 its origin in a preservation bias. The soil carbonates analyzed in this study developed in floodplain environments of post-11 Ma basins within low-relief fluvial and lacustrine settings that, similar to today, were interrupted by relict mountain ranges and local fault-controlled relief, but were not connected to marine basins. The floodplain records are currently accessible as a result of rapid latest Miocene to Pliocene drainage integration of the Anatolian plateau and subsequent river incision (Brocard et al., 2021; Meijers et al., 2020). Our soil carbonate $\delta^{13}C$ records are therefore biased towards partially preserved and incised
230 intermontane floodplains and underrepresent vegetation dynamics of (potentially) forested and eroding topographic highs. However, wind-blown pollen from forested montane areas are partially preserved in the floodplain areas. Our complementary $\delta^{13}C$ soil carbonate record therefore allows for the recognition of highly variable vegetation cover in Anatolia during the Late Miocene.

4.3 Timing and drivers of Late Miocene ecological change

Located at the crossroads of Africa, Asia, and Europe, the soil carbonate $\delta^{13}C$ record of Anatolia bears the potential to identify paleoenvironmental dynamics specific to the spread of C_4 vegetation in the Old World as well as to changing paleoclimatic conditions in the Mediterranean region. We compare the Anatolian soil carbonate $\delta^{13}C$ record with available leaf wax, fossil tooth enamel, and soil carbonate $\delta^{13}C$ records that constrain the initial expansion of C_4 vegetation (Polissar et al., 2019) and its rise to dominance in the Old World grasslands during the Late Miocene (Fig. 3d-f). We conclude that the onset of C_4 expansion in Anatolia during the Late Miocene (at the latest at ca. 9.9 Ma) is roughly coeval with the expansion of C_4 ecosystems in NW and E Africa and predates its rise in other Asian and African regions (Fig. 3f). However, C_4 vegetation dominated Anatolian floodplains and potentially parts of the Aegean by ca. 7.2 Ma, which roughly coincides with the timing of the rapid rise to dominance of C_4 vegetation in southern Asian grasslands between 8.0 and 4.7 Ma (Fig. 3c, d; e.g., Behrensmeyer et al., 2007; Quade and Cerling, 1995) and predates the rise to dominance of C_4 vegetation in the grasslands of the southern East African Rift during the Pliocene (Fig. 3e; e.g., Cerling et al., 2011; Lüdecke et al., 2016).

The rise to dominance of C_4 vegetation in East Asian grassland ecosystems is hypothesized to have occurred in response to declining atmospheric pCO_2 levels that led to Late Miocene Cooling (LMC, ca. 7.5 to 5.5 Ma; Fig. 3b; Herbert et al., 2016) when low pCO_2 provided an evolutionary advantage for C_4 over C_3 vegetation despite decreasing temperatures (e.g., Polissar et al., 2019; Wen et al., 2023). Worldwide, LMC is manifested in a sharp drop in sea surface temperatures (SSTs; Fig. 3b; (Herbert et al., 2016)) and its onset is accompanied by a sharp decrease in $\delta^{13}C$ values of benthic foraminifera (Fig. 3a; Westerhold et al., 2020), which attests to a profound change in the global carbon cycle and consequently ocean circulation patterns (Holbourn et al., 2018). Climatic reconstructions from Anatolia based on the coexistence approach (Supplementary Table S2) indicate a decrease in mean annual (ca. 2−3 °C) and particularly cold month mean temperatures (up to 10°C) during the Late Miocene, although uncertainties in both reconstructed temperatures and ages are large (see Fig. 2b, c). Because the rise to dominance of C_4 vegetation in Anatolian floodplains and possibly the Aegean occurred simultaneously with its rise in southern Asian ecosystems and LMC (Fig. 3c, d) we suggest that it was caused by drivers that go beyond regional environmental changes such as surface uplift of the CAP since ca. 11 Ma (Fig. 2d; Meijers et al., 2018).

Whereas C_4 grassland expansion in southern Asia, the Chinese Loess Plateau, and Arabia coincided with aridification (Huang et al., 2007; Wen et al., 2023), the (gradual) expansion of C_4 vegetation in northern and eastern Africa was not driven by aridification (Crocker et al., 2022; Polissar et al., 2019). The latter also appears to hold for Anatolia and the Aegean, as indicated by Anatolian paleobotanical datasets suggesting subhumid conditions (e.g., Kayseri-Özer, 2017; Supplementary Table S3) and mesic environments in Anatolia and the Aegean instead (Denk et al., 2018).

Around ca. 8.0−6.6 Ma, the Pikermian chronofauna peaked in terms of geographic extent (Fig. 2d), including large parts of Europe and Central Asia (Eronen et al., 2009). We suggest that the spread of C_4 grasslands, which started before 9.9 Ma, and their dominance in floodplain environments by 7.2 Ma led to the expansion of the hypsodont Pikermian chronofauna in Anatolia. A similar process is observed in southern Asian grasslands, where combined soil and fossil mammal tooth enamel

$\delta^{13}C$ values show that long-term climate forcing changed the vegetation structure (C_3 to C_4) between 8.5 and 6.0 Ma and led to the disappearance of most mammalian lineages that fed on C_3 vegetation (Badgley et al., 2008).

270

4.4 Drivers and consequences of unique and persistent Early Pliocene C_4 decline

A marked decrease in our pedogenic carbonate $\delta^{13}C$ values by approximately 7 ‰ from 4.9 to 3.9 Ma (Fig. 2a) implies a major overturn of Anatolian and potentially Aegean ecosystems. This transition led to the reemergence of landscapes dominated by C_3 vegetation, a feature that persists to the present day. Plant leaf wax $\delta^{13}C$ values and pollen data from a sediment core in the Gulf of Aden reveal a brief reversal in the trend of increasing C_4 vegetation contributions between 4.9 and 4.6 Ma (Feakins et al., 2013). On and around the Chinese Loess Plateau, variations in C_4 and C_3 biomass have been linked to the strengthening and weakening of the East Asian summer monsoon (e.g., An et al., 2005; Passey et al., 2009; Yao et al., 2010). However, these fluctuations are not persistent over time. Therefore, the rapid and persistent Pliocene switch to C_3 vegetation is a feature that is unique to Anatolia. By contrast, southeast China (Fig. 3f) and regions in the New World (see e.g., Polissar et al., 2019) have been colonized by C_4 vegetation only after the return to C_3-dominated vegetation in Anatolia. Given that the return to C_3 vegetation is geographically limited we assess potential causes for C_4 decline in Anatolia within a regional framework.

The Messinian Salinity Crisis (MSC) in the Mediterranean basin (5.96−5.33 Ma; e.g., Roveri et al., 2014) had the potential to alter the regional hydrologic cycle and hence vegetation. However, considering that the MSC is relatively short-lived and predates the decline of C_4 grasslands in Anatolia between 4.9 and 3.9 Ma, it is unlikely to be the main driver of the prolonged changes in the vegetation structure of the Eastern Mediterranean region.

During the Early Pliocene, regions adjacent to Anatolia also experienced significant environmental changes. In Central Europe, increased aridity led to the disappearance of open woodland, broad-leaf evergreen, and humid sclerophyllous taxa (Mosbrugger et al., 2005), some of which found refuge in Anatolia and the Eastern Mediterranean region (Eronen et al., 2009). Concurrently, Eastern Europe experienced a transition to cooler, drier conditions, leading to the expansion of grasslands and an enhanced fire regime since ca. 4.4 Ma (Feurdean and Vasiliev, 2019). The divergence in climate between a drier Central Europe and a more humid Eastern Mediterranean region (Kovar-Eder, 2003) has been attributed to the deflection of the westerlies from Central Europe to the Mediterranean region (Eronen et al., 2009). Its timing coincides with strengthening of the Atlantic Meridional Overturning Circulation (AMOC) in response to shoaling of the Central American Seaway (CAS) around 4.8−4.0 Ma (e.g., Haug and Tiedemann, 1998). We therefore surmise that the increase in SSTs over the North Atlantic associated with AMOC strengthening (Karas et al., 2017) caused hydroclimatic changes over Europe and the Mediterranean region.
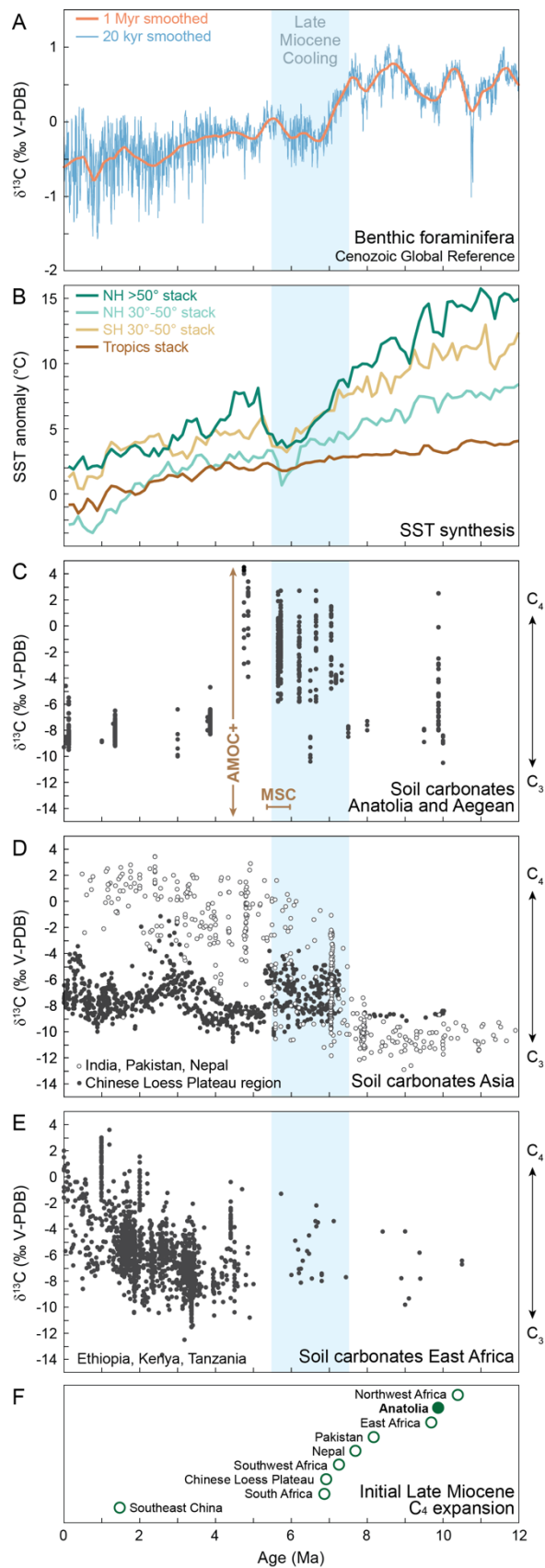
Climate
of the Past
Discussions

Figure 3. Climate and carbon isotope records spanning the last 12 Ma. (a) Cenozoic Global Reference (CENOGRID) benthic foraminifera
300 $\delta^{13}C$ curves, resampled and smoothed over 20 kyr (blue) and 1 Myr (red) periods (Westerhold et al., 2020). (b) SST anomalies for different
hemispheric and latitude bins (Herbert et al., 2016). C−E: Compilation of soil carbonate $\delta^{13}C$ values from Anatolia and the Aegean (c), Asia
(d), and Africa (e). Asian and African datasets were retrieved from Fox et al. (2018). See Sect. 2.5. (f) Onset of the initial C_4 expansion in
the Old World from a compilation by Polissar et al. (2019) and including Anatolia (this study). Blue shading indicates time interval of Late
Miocene Cooling (Herbert et al., 2016). NH= Northern Hemisphere, SH= Southern Hemisphere. MSC: Messinian Salinity Crisis; AMOC+:
305 strengthened AMOC (see Sect. 4.4).

Regions with prevalent C_4 vegetation today are not only characterized by high growing season temperatures but also
by warm season precipitation. In contrast, Anatolia presently experiences hot, dry Mediterranean summers and receives most
of its precipitation from October through May (Schemmel et al., 2013; Türkeş and Erlat, 2005). Notably, leaf morphologies of
310 Miocene species of evergreen oak (*Quercus* sect. *Ilex*) from southwest Türkiye and Aegean islands resemble modern
Himalayan members, which suggests (summer-)humid climatic conditions (see Denk et al. (2018), but also Denk et al. (2014)
and Velitzelos et al. (2014)). Additionally, Tortonian (ca. 11.6−7.2 Ma) paleoclimate simulations of Europe indicate humid to
subhumid summer conditions in the northern Mediterranean region (Quan et al., 2014). We therefore propose that the shift
from warm to cold season precipitation and the emergence of a Mediterranean-style climate drove the demise of C_4 grasslands
315 and a return to a C_3-dominated environment in Anatolia and the Aegean during the Early Pliocene (4.9 to 3.9 Ma).

The Early Pliocene demise of C_4 biomass occurred simultaneously with significant large mammal faunal turnover
(Huang et al., 2019) and the vanishing of open-landscape adapted large mammals from Anatolia (MN14; Eronen et al., 2009),
which formed the last stronghold of the Pikermian chronofauna (Eronen et al., 2009). Our study therefore identifies long-term
vegetation dynamics and indicates that Early Pliocene climate change profoundly and irreversibly transformed vegetation
320 structures and drove a turnover in mammalian populations.

5. Conclusions

C_4 vegetation became ecologically dominant in Anatolian grasslands by 7.2 Ma, contemporaneous with similar developments
in southern Asia and the Aegean. In contrast to the common association of C_4 biomass expansion with arid conditions as the
325 main driver, however, C_4 expansion in Anatolia occurred under relatively humid conditions as indicated by consistent
paleobotanical and stable isotope paleoclimate records. This suggests that a reduction in atmospheric pCO_2 between ca. 7.5
and 5.5 Ma primarily drove C_4 expansion in this region. A distinctive, rapid decline of C_4 vegetation is observed in Anatolia
between 4.9 and 3.9 Ma, leading to a C_3 vegetation-dominated environment that has persisted until today. We hypothesize that
this shift, along with the disappearance of the Pikermian chronofauna, was influenced by the transition to a Mediterranean
330 climate characterized by a change from warm to cold season precipitation.

Data availability. All supporting datasets are available as Supplementary information files that will be freely accessible upon publication.

335 **Author contributions:** MJM, TM, and AM: Conceptualization; MJM and TM: Investigation; MJM, TM, TL, AM: Methodology; MJM, TM, BR, HEÇ, EA, TL, and AM: Resources; MJM: Visualization; MJM: Writing – original draft; MJM, TM, BR, HEÇ, EA, TL, and AM: Writing – review & editing.

Competing interests. The authors declare that they have no conflict of interest.

340

References

350 An, Z., Huang, Y., Liu, W., Guo, Z., Clemens, S., Li, L., Prell, W., Ning, Y., Cai, Y., Zhou, W., Lin, B., Zhang, Q., Cao, Y., Qiang, X., Chang, H., and Wu, Z.: Multiple expansions of C4 plant biomass in East Asia since 7 Ma coupled with strengthened monsoon circulation, Geology, 33, 705–708, https://doi.org/10.1130/G21423.1, 2005.

Aronson, J., Hailemichael, M., and Savin, S.: Hominid environments at Hadar from paleosol studies in a framework of Ethiopian climate change, J Hum Evol, 55, 532–550, https://doi.org/10.1016/j.jhevol.2008.04.004, 2008.

355 Aydar, E., Schmitt, A. K., Çubukçu, H. E., Akin, L., Ersoy, O., Sen, E., Duncan, R. A., and Atici, G.: Correlation of ignimbrites in the central Anatolian volcanic province using zircon and plagioclase ages and zircon compositions, Journal of Volcanology and Geothermal Research, 213–214, 83–97, https://doi.org/10.1016/j.jvolgeores.2011.11.005, 2012.

Badgley, C., Barry, J. C., Le, M., Morgan, E., Nelson, S. V, Behrensmeyer, A. K., Cerling, T. E., and Pilbeam, D.: Ecological changes in Miocene mammalian record show impact of prolonged climatic forcing, 2008.

360 Behrensmeyer, A. K., Quade, J., Cerling, T. E., Kappelman, J., Khan, I. A., Copeland, P., Roe, L., Hicks, J., Stubblefield, P., Willis, B. J., and Latorre, C.: The structure and rate of late Miocene expansion of C4 plants: Evidence from lateral variation in stable isotopes in paleosols of the Siwalik Group, northern Pakistan, Bulletin of the Geological Society of America, 119, 1486–1505, https://doi.org/10.1130/B26064.1, 2007.

Bernor, R. L., Mirzaie Ataabadi, M., Meshida, K., and Wolf, D.: The Maragheh hipparions, late Miocene of Azarbaijan, Iran,

365 Paleobiodivers Paleoenviron, 96, 453–488, https://doi.org/10.1007/s12549-016-0235-2, 2016.

Bestland, E. A. and Krull, E. S.: Palaeoenvironments of Early Miocene Kisingiri volcano Proconsul sites: evidence from carbon isotopes, palaeosols and hydromagmatic deposits, J Geol Soc London, 156, 965–976, https://doi.org/10.1144/gsjgs.156.5.0965, 1999.

370 Biasatti, D., Bernor, R. L., and Cooper, L. W.: Insights on Late Miocene climate change and regional uplift in Maragheh Basin, eastern Azerbaijan Province, northwest Iran revealed by stable carbon and oxygen isotope analyses of fossil horse tooth enamel, in: 75th Annual Meeting, Society of Vertebrate Paleontology, 89–89, 2015.

Böhme, M., Spassov, N., Ebner, M., Geraads, D., Hristova, L., Kirscher, U., Kötter, S., Linnemann, U., Prieto, J., Roussiakis, S., Theodorou, G., Uhlig, G., and Winklhofer, M.: Messinian age & savannah environment of the possible hominin Graecopithecus from Europe, PLoS One, 12, https://doi.org/10.1371/journal.pone.0177347, 2017.

375 Böhme, M., Spassov, N., Majidifard, M. R., Gärtner, A., Kirscher, U., Marks, M., Dietzel, C., Uhlig, G., El Atfy, H., Begun, D. R., and Winklhofer, M.: Neogene hyperaridity in Arabia drove the directions of mammalian dispersal between Africa and Eurasia, Commun Earth Environ, 2, 85, https://doi.org/10.1038/s43247-021-00158-y, 2021.

Brocard, G. Y., Meijers, M. J. M., Cosca, M. A., Salles, T., Willenbring, J., Teyssier, C., and Whitney, D. L.: Fast Pliocene integration of the Central Anatolian Plateau drainage: Evidence, processes, and driving forces, Geosphere, 17, 739–765, 380 https://doi.org/10.1130/GES02247.1, 2021.

Butiseacă, G. A., van der Meer, M. T. J., Kontakiotis, G., Agiadi, K., Thivaiou, D., Besiou, E., Antonarakou, A., Mulch, A., and Vasiliev, I.: Multiple crises preceded the Mediterranean Salinity Crisis: Aridification and vegetation changes revealed by biomarkers and stable isotopes, Glob Planet Change, 217, https://doi.org/10.1016/j.gloplacha.2022.103951, 2022.

Caves, J. K., Moragne, D. Y., Ibarra, D. E., Bayshashov, B. U., Gao, Y., Jones, M. M., Zhamangara, A., Arzhannikova, A. V., 385 Arzhannikov, S. G., and Chamberlain, C. P.: The Neogene de-greening of Central Asia, Geology, 44, 887–890, https://doi.org/10.1130/G38267.1, 2016.

Cerling, T. E.: The stable isotopic composition of modern soil carbonate and its relationship to climate, Earth and Planetary Science Letters, 229–240 pp., 1984.

Cerling, T. E. and Hay, R. L.: An Isotopic Study of Paleosol Carbonates from Olduvai Gorge, Quat Res, 25, 63–78, 390 https://doi.org/10.1016/0033-5894(86)90044-X, 1986.

Cerling, T. E. and Quade, J.: Stable Carbon and Oxygen Isotopes in Soil Carbonates, in: Geophysical Monograph, vol. 78, 217–231, https://doi.org/10.1029/GM078p0217, 1993.

Cerling, T. E., Bowman, J. R., and O'Neil, J. R.: An isotopic study of a fluvial-lacustrine sequence: The Plio-Pleistocene koobi fora sequence, East Africa, Palaeogeogr Palaeoclimatol Palaeoecol, 63, 335–356, https://doi.org/10.1016/0031-395 0182(88)90104-6, 1988.

Cerling, T. E., Quade, J., Ambrose, S. H., and Sikes, N. E.: Fossil soils, grasses, and carbon isotopes from Fort Ternan, Kenya: grassland or woodland?, J Hum Evol, 21, 295–306, https://doi.org/10.1016/0047-2484(91)90110-H, 1991.

Cerling, T. E., Harris, J. M., MacFadden, B. J., Leakey, M. G., Quadek, J., Eisenmann, V., and Ehleringer, J. R.: Global vegetation change through the Miocene/Pliocene boundary, Nature © Macmillan Publishers Ltd, 1997.

400   Cerling, T. E., Harris, J. M., and Leakey, M. G.: 12.2. Isotope Paleoecology of the Nawata and Nachukui Formations at Lothagam, Turkana Basin, Kenya, in: Lothagam, Columbia University Press, 605–624, https://doi.org/10.7312/leak11870-024, 2003.

Cerling, T. E., Wynn, J. G., Andanje, S. A., Bird, M. I., Korir, D. K., Levin, N. E., Mace, W., Macharia, A. N., Quade, J., and Remien, C. H.: Woody cover and hominin environments in the past 6 million years, Nature, 476, 51–56,
405   https://doi.org/10.1038/nature10306, 2011.

Crocker, A. J., Naafs, B. D. A., Westerhold, T., James, R. H., Cooper, M. J., Röhl, U., Pancost, R. D., Xuan, C., Osborne, C. P., Beerling, D. J., and Wilson, P. A.: Astronomically controlled aridity in the Sahara since at least 11 million years ago, Nat Geosci, 15, 671–676, https://doi.org/10.1038/s41561-022-00990-7, 2022.

Denk, T., Güner, T. H., and Grimm, G. W.: From mesic to arid: Leaf epidermal features suggest preadaptation in Miocene
410   dragon trees (Dracaena), Rev Palaeobot Palynol, 200, 211–228, https://doi.org/10.1016/j.revpalbo.2013.09.009, 2014.

Denk, T., Zohner, C. M., Grimm, G. W., and Renner, S. S.: Plant fossils reveal major biomes occupied by the late Miocene Old-World Pikermian fauna, Nat Ecol Evol, 2, 1864–1870, https://doi.org/10.1038/s41559-018-0695-z, 2018.

Ding, Z. L. and Yang, S. L.: C3/C4 vegetation evolution over the last 7.0 Myr in the Chinese Loess Plateau: evidence from pedogenic carbonate δ13C, Palaeogeogr Palaeoclimatol Palaeoecol, 160, 291–299, https://doi.org/10.1016/S0031-
415   0182(00)00076-6, 2000.

Edwards, E. J., Osborne, C. P., Strömberg, C. A. E., Smith, S. A., Bond, W. J., Christin, P. A., Cousins, A. B., Duvall, M. R., Fox, D. L., Freckleton, R. P., Ghannoum, O., Hartwell, J., Huang, Y., Janis, C. M., Keeley, J. E., Kellogg, E. A., Knapp, A. K., Leakey, A. D. B., Nelson, D. M., Saarela, J. M., Sage, R. F., Sala, O. E., Salamin, N., Still, C. J., and Tipple, B.: The origins of C4 Grasslands: Integrating evolutionary and ecosystem science, https://doi.org/10.1126/science.1177216, 30 April
420   2010.

Eronen, J. T., Ataabadi, M. M., Micheels, A., Karme, A., Bernor, R. L., and Fortelius, M.: Distribution history and climatic controls of the Late Miocene Pikermian chronofauna, Proc Natl Acad Sci U S A, 106, 11867–11871, https://doi.org/10.1073/pnas.0902598106, 2009.

Feakins, S. J., Levin, N. E., Liddy, H. M., Sieracki, A., Eglinton, T. I., and Bonnefille, R.: Northeast african vegetation change
425   over 12 m.y, Geology, 41, 295–298, https://doi.org/10.1130/G33845.1, 2013.

Feurdean, A. and Vasiliev, I.: The contribution of fire to the late Miocene spread of grasslands in eastern Eurasia (Black Sea region), Sci Rep, 9, https://doi.org/10.1038/s41598-019-43094-w, 2019.

Fortelius, M., Bibi, F., Tang, H., Žliobaitė, I., Eronen, J. T., and Kaya, F.: The nature of the Old World savannah palaeobiome, https://doi.org/10.1038/s41559-019-0857-7, 1 April 2019.

430   Fox, D. L., Pau, S., Taylor, L., Strömberg, C. A. E., Osborne, C. P., Bradshaw, C., Conn, S., Beerling, D. J., and Still, C. J.: Climatic Controls on C4 Grassland Distributions During the Neogene: A Model-Data Comparison, Front Ecol Evol, 6, https://doi.org/10.3389/fevo.2018.00147, 2018.

Ghosh, P., Padia, J. T., and Mohindra, R.: Stable isotopic studies of palaeosol sediment from Upper Siwalik of Himachal Himalaya: Evidence for high monsoonal intensity during late Miocene?, Palaeogeogr Palaeoclimatol Palaeoecol, 206, 103–114, https://doi.org/10.1016/j.palaeo.2004.01.014, 2004.

Haug, G. H. and Tiedemann, R.: Effect of the formation of the Isthmus of Panama on Atlantic Ocean thermohaline circulation, Nature, 393, 673–676, https://doi.org/10.1038/31447, 1998.

Herbert, T. D., Lawrence, K. T., Tzanova, A., Peterson, L. C., Caballero-Gill, R., and Kelly, C. S.: Late Miocene global cooling and the rise of modern ecosystems, Nat Geosci, 9, 843–847, https://doi.org/10.1038/ngeo2813, 2016.

Holbourn, A. E., Kuhnt, W., Clemens, S. C., Kochhann, K. G. D., Jöhnck, J., Lübbers, J., and Andersen, N.: Late Miocene climate cooling and intensification of southeast Asian winter monsoon, Nat Commun, 9, 1584, https://doi.org/10.1038/s41467-018-03950-1, 2018.

Huang, S., Meijers, M. J. M., Eyres, A., Mulch, A., and Fritz, S. A.: Unravelling the history of biodiversity in mountain ranges through integrating geology and biogeography, J Biogeogr, 46, 1777–1791, https://doi.org/10.1111/jbi.13622, 2019.

Huang, Y., Clemens, S. C., Liu, W., Wang, Y., and Prell, W. L.: Large-scale hydrological change drove the late Miocene C4 plant expansion in the Himalayan foreland and Arabian Peninsula, Geology, 35, 531, https://doi.org/10.1130/G23666A.1, 2007.

Kaakinen, A., Sonninen, E., and Lunkka, J. P.: Stable isotope record in paleosol carbonates from the Chinese Loess Plateau: Implications for late Neogene paleoclimate and paleovegetation, Palaeogeogr Palaeoclimatol Palaeoecol, 237, 359–369, https://doi.org/10.1016/j.palaeo.2005.12.011, 2006.

Karas, C., Nürnberg, D., Bahr, A., Groeneveld, J., Herrle, J. O., Tiedemann, R., and Demenocal, P. B.: Pliocene oceanic seaways and global climate, Sci Rep, 7, https://doi.org/10.1038/srep39842, 2017.

Kaya, F., Bibi, F., Žliobaite, I., Eronen, J. T., Hui, T., and Fortelius, M.: The rise and fall of the Old World savannah fauna and the origins of the African savannah biome, Nat Ecol Evol, 2, 241–246, https://doi.org/10.1038/s41559-017-0414-1, 2018.

Kayseri-Özer, M. S.: Cenozoic vegetation and climate change in Anatolia — A study based on the IPR-vegetation analysis, Palaeogeogr Palaeoclimatol Palaeoecol, 467, 37–68, https://doi.org/10.1016/j.palaeo.2016.10.001, 2017.

Kayseri-Özer, M. S., Karadenizli, L., Akgün, F., Oyal, N., Saraç, G., Şen, Ş., Tunoğlu, C., and Tuncer, A.: Palaeoclimatic and palaeoenvironmental interpretations of the Late Oligocene, Late Miocene–Early Pliocene in the Çankırı-Çorum Basin, Palaeogeogr Palaeoclimatol Palaeoecol, 467, 16–36, https://doi.org/10.1016/j.palaeo.2016.05.022, 2017.

Kingston, J.: Stable isotopic evidence for hominid paleoenvironments in East Africa, PhD Thesis, Harvard University, 1–162 pp., 1992.

Kohn, M. J.: Carbon isotope compositions of terrestrial C3 plants as indicators of (paleo)ecology and (paleo)climate, GEOLOGY ECOLOGY, 107, 19691–19695, https://doi.org/10.1073/pnas.1004933107/-/DCSupplemental, 2010.

Kovar-Eder, J.: Vegetation dynamics in Europe during the Neogene, in: Distribution and Migration of Tertiary Mammals in Eurasia. A volume in Honour of Hans de Bruijn., edited by: Reumer, J. W. F. and Wessels, W., DEINSEA, Rotterdam, 373–392, 2003.

Lepetit, P.: Kohlenstoff-Isotopie miozäner Calcretes in Kappadokien (Türkei), PhD Thesis, Friedrich-Schiller-Universität Jena, Jena, 1–218 pp., 2010.

Levin, N. E., Quade, J., Simpson, S. W., Semaw, S., and Rogers, M.: Isotopic evidence for Plio–Pleistocene environmental change at Gona, Ethiopia, Earth Planet Sci Lett, 219, 93–110, https://doi.org/10.1016/S0012-821X(03)00707-6, 2004.

Levin, N. E., Brown, F. H., Behrensmeyer, A. K., Bobe, R., and Cerling, T. E.: Paleosol carbonates from the Omo Group: Isotopic records of local and regional environmental change in East Africa, Palaeogeogr Palaeoclimatol Palaeoecol, 307, 75–89, https://doi.org/10.1016/j.palaeo.2011.04.026, 2011.

Licht, A., Dupont-Nivet, G., Meijer, N., Caves Rugenstein, J., Schauer, A., Fiebig, J., Mulch, A., Hoorn, C., Barbolini, N., and Guo, Z.: Decline of soil respiration in northeastern Tibet through the transition into the Oligocene icehouse, Palaeogeogr Palaeoclimatol Palaeoecol, 560, https://doi.org/10.1016/j.palaeo.2020.110016, 2020.

Lüdecke, T., Schrenk, F., Thiemeyer, H., Kullmer, O., Bromage, T. G., Sandrock, O., Fiebig, J., and Mulch, A.: Persistent C3 vegetation accompanied Plio-Pleistocene hominin evolution in the Malawi Rift (Chiwondo Beds, Malawi), J Hum Evol, 90, 163–175, https://doi.org/10.1016/j.jhevol.2015.10.014, 2016.

Mayser, J. P., Flecker, R., Marzocchi, A., Kouwenhoven, T. J., Lunt, D. J., and Pancost, R. D.: Precession driven changes in terrestrial organic matter input to the Eastern Mediterranean leading up to the Messinian Salinity Crisis, Earth Planet Sci Lett, 462, 199–211, https://doi.org/10.1016/j.epsl.2017.01.029, 2017.

Meijers, M. J. M., Brocard, G. Y., Cosca, M. A., Lüdecke, T., Teyssier, C., Whitney, D. L., and Mulch, A.: Rapid late Miocene surface uplift of the Central Anatolian Plateau margin, Earth Planet Sci Lett, 497, 29–41, https://doi.org/10.1016/j.epsl.2018.05.040, 2018.

Meijers, M. J. M., Brocard, G. Y., Whitney, D. L., and Mulch, A.: Paleoenvironmental conditions and drainage evolution of the central Anatolian lake system (Turkey) during Late Miocene to Pliocene surface uplift, Geosphere, 16, 490–509, https://doi.org/10.1130/GES02135.1, 2020.

Mosbrugger, V. and Utescher, T.: The coexistence approach — a method for quantitative reconstructions of Tertiary terrestrial palaeoclimate data using plant fossils, Palaeogeogr Palaeoclimatol Palaeoecol, 134, 61–86, https://doi.org/10.1016/S0031-0182(96)00154-X, 1997.

Mosbrugger, V., Utescher, T., and Dilcher, D. L.: Cenozoic continental climatic evolution of Central Europe, 2005.

Özsayin, E., Çiner, T. A., Rojay, F. B., Dirik, R. K., Melnick, D., Fernandez-Blanco, D., Bertotti, G., Schildgen, T. F., Garcin, Y., Strecker, M. R., and Sudo, M.: Plio-Quaternary extensional tectonics of the Central Anatolian Plateau: a case study from the Tuz Gölü Basin, Turkey, Turkish Journal of Earth Sciences, https://doi.org/10.3906/yer-1210-5, 2013.

Passey, B. H., Ayliffe, L. K., Kaakinen, A., Zhang, Z., Eronen, J. T., Zhu, Y., Zhou, L., Cerling, T. E., and Fortelius, M.: Strengthened East Asian summer monsoons during a period of high-latitude warmth? Isotopic evidence from Mio-Pliocene fossil mammals and soil carbonates from northern China, Earth Planet Sci Lett, 277, 443–452, https://doi.org/10.1016/j.epsl.2008.11.008, 2009.

500   Peppe, D. J., Cote, S. M., Deino, A. L., Fox, D. L., Kingston, J. D., Kinyanjui, R. N., Lukens, W. E., MacLatchy, L. M.,
      Novello, A., Strömberg, C. A. E., Driese, S. G., Garrett, N. D., Hillis, K. R., Jacobs, B. F., Jenkins, K. E. H., Kityo, R. M.,
      Lehmann, T., Manthi, F. K., Mbua, E. N., Michel, L. A., Miller, E. R., Mugume, A. A. T., Muteti, S. N., Nengo, I. O., Oginga,
      K. O., Phelps, S. R., Polissar, P., Rossie, J. B., Stevens, N. J., Uno, K. T., and McNulty, K. P.: Oldest evidence of abundant
      C4 grasses and habitat heterogeneity in eastern Africa, Science (1979), 380, 173–177,
505   https://doi.org/10.1126/science.abq2834, 2023.

      Plummer, T., Bishop, L. C., Ditchfield, P., and Hicks, J.: Research on Late Pliocene Oldowan Sites at Kanjera South, Kenya,
      J Hum Evol, 36, 151–170, https://doi.org/10.1006/jhev.1998.0256, 1999.

      Plummer, T. W., Ditchfield, P. W., Bishop, L. C., Kingston, J. D., Ferraro, J. V., Braun, D. R., Hertel, F., and Potts, R.: Oldest
      Evidence of Toolmaking Hominins in a Grassland-Dominated Ecosystem, PLoS One, 4, e7199,
510   https://doi.org/10.1371/journal.pone.0007199, 2009.

      Polissar, P. J., Rose, C., Uno, K. T., Phelps, S. R., and deMenocal, P.: Synchronous rise of African C4 ecosystems 10 million
      years ago in the absence of aridification, Nat Geosci, 12, 657–660, https://doi.org/10.1038/s41561-019-0399-2, 2019.

      Quade, J. and Cerling, T. E.: Expansion of C4 grasses in the Late Miocene of Northern Pakistan: evidence from stable isotopes
      in paleosols, Palaeogeogr Palaeoclimatol Palaeoecol, 115, 91–116, https://doi.org/10.1016/0031-0182(94)00108-K, 1995.

515   Quade, J., Solounias, N., and Cerling, T. E.: Stable isotopic evidence from paleosol carbonates and fossil teeth in Greece for
      forest or woodlands over the past 11 Ma, Palaeogeogr Palaeoclimatol Palaeoecol, 108, 41–53, https://doi.org/10.1016/0031-
      0182(94)90021-3, 1994.

      Quade, J., Levin, N., Semaw, S., Stout, D., Renne, P., Rogers, M., and Simpson, S.: Paleoenvironments of the earliest stone
      toolmakers, Gona, Ethiopia, Geol Soc Am Bull, 116, 1529–1544, https://doi.org/10.1130/B25358.1, 2004.

520   Quan, C., Liu, Y. S. C., Tang, H., and Utescher, T.: Miocene shift of European atmospheric circulation from trade wind to
      westerlies, Sci Rep, 4, https://doi.org/10.1038/srep05660, 2014.

      Quinn, R. L., Lepre, C. J., Wright, J. D., and Feibel, C. S.: Paleogeographic variations of pedogenic carbonate δ13C values
      from Koobi Fora, Kenya: implications for floral compositions of Plio-Pleistocene hominin environments, J Hum Evol, 53,
      560–573, https://doi.org/10.1016/j.jhevol.2007.01.013, 2007.

525   Rey, K., Amiot, R., Lécuyer, C., Koufos, G. D., Martineau, F., Fourel, F., Kostopoulos, D. S., and Merceron, G.: Late Miocene
      climatic and environmental variations in northern Greece inferred from stable isotope compositions (δ18O, δ13C) of equid
      teeth apatite, Palaeogeogr Palaeoclimatol Palaeoecol, 388, 48–57, https://doi.org/10.1016/j.palaeo.2013.07.021, 2013.

      Roveri, M., Flecker, R., Krijgsman, W., Lofi, J., Lugli, S., Manzi, V., Sierro, F. J., Bertini, A., Camerlenghi, A., De Lange,
      G., Govers, R., Hilgen, F. J., Hübscher, C., Meijer, P. T., and Stoica, M.: The Messinian Salinity Crisis: Past and future of a
530   great challenge for marine sciences, Mar Geol, 352, 25–58, https://doi.org/10.1016/j.margeo.2014.02.002, 2014.

      Sage, R. F.: The evolution of C 4 photosynthesis, New Phytologist, 161, 341–370, https://doi.org/10.1046/j.1469-
      8137.2004.00974.x, 2004.

Sahnouni, M., Van der Made, J., and Everett, M.: Ecological background to Plio-Pleistocene hominin occupation in North Africa: the vertebrate faunas from Ain Boucherit, Ain Hanech and El-Kherba, and paleosol stable-carbon-isotope studies from

535 El-Kherba, Algeria, Quat Sci Rev, 30, 1303–1317, https://doi.org/10.1016/j.quascirev.2010.01.002, 2011.

Sanyal, P., Bhattacharya, S. K., Kumar, R., Ghosh, S. K., and Sangode, S. J.: Mio-Pliocene monsoonal record from Himalayan foreland basin (Indian Siwalik) and its relation to vegetational change, Palaeogeogr Palaeoclimatol Palaeoecol, 205, 23–41, https://doi.org/10.1016/j.palaeo.2003.11.013, 2004.

Schemmel, F., Mikes, T., Rojay, B., and Mulch, A.: The impact of topography on isotopes in precipitation across the central

540 Anatolian plateau (Turkey), Am J Sci, 313, 61–80, https://doi.org/10.2475/02.2013.01, 2013.

Sikes, N. E.: Early hominid habitat preferences in East Africa: Paleosol carbon isotopic evidence, J Hum Evol, 27, 25–45, https://doi.org/10.1006/jhev.1994.1034, 1994.

Sikes, N. E. and Ashley, G. M.: Stable isotopes of pedogenic carbonates as indicators of paleoecology in the Plio-Pleistocene (upper Bed I), western margin of the Olduvai Basin, Tanzania, J Hum Evol, 53, 574–594,

545 https://doi.org/10.1016/j.jhevol.2006.12.008, 2007.

Sikes, N. E., Potts, R., and Behrensmeyer, A. K.: Early Pleistocene habitat in Member 1 Olorgesailie based on paleosol stable isotopes, J Hum Evol, 37, 721–746, https://doi.org/10.1006/jhev.1999.0343, 1999.

Spötl, C. and Vennemann, T. W.: Continuous-flow isotope ratio mass spectrometric analysis of carbonate minerals, Rapid Communications in Mass Spectrometry, 17, 1004–1006, https://doi.org/10.1002/rcm.1010, 2003.

550 Still, C. J., Berry, J. A., Collatz, G. J., and DeFries, R. S.: Global distribution of C3 and C4 vegetation: Carbon cycle implications, Global Biogeochem Cycles, 17, https://doi.org/10.1029/2001gb001807, 2003.

Strömberg, C. A. E.: Evolution of grasses and grassland ecosystems, Annu Rev Earth Planet Sci, 39, 517–544, https://doi.org/10.1146/annurev-earth-040809-152402, 2011.

Strömberg, C. A. E., Werdelin, L., Friis, E. M., and Saraç, G.: The spread of grass-dominated habitats in Turkey and

555 surrounding areas during the Cenozoic: Phytolith evidence, Palaeogeogr Palaeoclimatol Palaeoecol, 250, 18–49, https://doi.org/10.1016/j.palaeo.2007.02.012, 2007.

Tipple, B. J. and Pagani, M.: The early origins of terrestrial C4 photosynthesis, Annu Rev Earth Planet Sci, 35, 435–461, https://doi.org/10.1146/annurev.earth.35.031306.140150, 2007.

Türkeş, M. and Erlat, E.: Climatological responses of winter precipitation in Turkey to variability of the North Atlantic

560 Oscillation during the period 1930-2001, Theor Appl Climatol, 81, 45–69, https://doi.org/10.1007/s00704-004-0084-1, 2005.

Ulu, Ü.: 1:500.000 Geological Map of Turkey, Adana, 2002.

Uno, K. T., Cerling, T. E., Harris, J. M., Kunimatsu, Y., Leakey, M. G., Nakatsukasa, M., and Nakaya, H.: Late Miocene to Pliocene carbon isotope record of differential diet change among East African herbivores, Proc Natl Acad Sci U S A, 108, 6509–6514, https://doi.org/10.1073/pnas.1018435108, 2011.

Climate
of the Past
Discussions

565 Urban, M. A., Nelson, D. M., Jimenez-Moreno, G., Chateauneuf, J.-J., Pearson, A., and Hu, F. S.: Isotopic evidence of C4 grasses in southwestern Europe during the Early Oligocene-Middle Miocene, Geology, 38, 1091–1094, https://doi.org/10.1130/G31117.1, 2010.

Velitzelos, D., Bouchal, J. M., and Denk, T.: Review of the Cenozoic floras and vegetation of Greece, https://doi.org/10.1016/j.revpalbo.2014.02.006, 2014.

570 Wen, Y., Zhang, L., Holbourn, A. E., Zhu, C., Huntington, K. W., Jin, T., Li, Y., and Wang, C.: CO2-forced Late Miocene cooling and ecosystem reorganizations in East Asia, Proc Natl Acad Sci U S A, 120, https://doi.org/10.1073/pnas.2214655120, 2023.

Westerhold, T., Marwan, N., Drury, A. J., Liebrand, D., Agnini, C., Anagnostou, E., Barnet, J. S. K., Bohaty, S. M., De Vleeschouwer, D., Florindo, F., Frederichs, T., Hodell, D. A., Holbourn, A. E., Kroon, D., Lauretano, V., Littler, K., Lourens,

575 L. J., Lyle, M., Pälike, H., Röhl, U., Tian, J., Wilkens, R. H., Wilson, P. A., and Zachos, J. C.: An astronomically dated record of Earth's climate and its predictability over the last 66 million years, Science (1979), 369, 1383–1387, https://doi.org/10.1126/science.aba6853, 2020.

WoldeGabriel, G., Ambrose, S. H., Barboni, D., Bonnefille, R., Bremond, L., Currie, B., DeGusta, D., Hart, W. K., Murray, A. M., Renne, P. R., Jolly-Saad, M. C., Stewart, K. M., and White, T. D.: The Geological, Isotopic, Botanical, Invertebrate,

580 and Lower Vertebrate Surroundings of Ardipithecus ramidus, Science (1979), 326, 65, https://doi.org/10.1126/science.1175817, 2009.

Wynn, J. G.: Paleosols, stable carbon isotopes, and paleoenvironmental interpretation of Kanapoi, Northern Kenya, J Hum Evol, 39, 411–432, https://doi.org/10.1006/jhev.2000.0431, 2000.

Wynn, J. G.: Influence of Plio-Pleistocene aridification on human evolution: Evidence from paleosols of the Turkana Basin,

585 Kenya, Am J Phys Anthropol, 123, 106–118, https://doi.org/10.1002/ajpa.10317, 2004.

Wynn, J. G., Alemseged, Z., Bobe, R., Geraads, D., Reed, D., and Roman, D. C.: Geological and palaeontological context of a Pliocene juvenile hominin at Dikika, Ethiopia, Nature, 443, 332–336, https://doi.org/10.1038/nature05048, 2006.

Yao, Z., Xiao, G., Wu, H., Liu, W., and Chen, Y.: Plio-Pleistocene vegetation changes in the North China Plain: Magnetostratigraphy, oxygen and carbon isotopic composition of pedogenic carbonates, Palaeogeogr Palaeoclimatol

590 Palaeoecol, 297, 502–510, https://doi.org/10.1016/j.palaeo.2010.09.003, 2010.

Zamanian, K., Pustovoytov, K., and Kuzyakov, Y.: Pedogenic carbonates: Forms and formation processes, https://doi.org/10.1016/j.earscirev.2016.03.003, 1 June 2016.

Zhuang, G., Hourigan, J. K., Koch, P. L., Ritts, B. D., and Kent-Corson, M. L.: Isotopic constraints on intensified aridity in Central Asia around 12Ma, Earth Planet Sci Lett, 312, 152–163, https://doi.org/10.1016/j.epsl.2011.10.005, 2011.

595